Desalination and Water Treatment
www.deswater.com

doi: 10.5004/dwt.2021.26721

213 (2021) 348–357
February

High-performance removal of iron from aqueous solution using modified activated carbon prepared from corn cobs and luffa sponge

Nohier El-Bendary, Hisham Kh. El-Etriby, Hani Mahanna*

Faculty of Engineering, Public Works Engineering Department, Mansoura University, Mansoura 35516, Egypt, emails: Hany_mss@mans.edu.eg (H. Mahanna), nohierelbendary@gmail.com (N. El-Bendary), eletribyhk@yahoo.com (H.K. El-Etriby)

Received 25 April 2020; Accepted 17 October 2020

ABSTRACT

Activated carbon prepared from corn cobs (CAC) and luffa sponge (LAC) modified with aluminum chloride (Al-CAC and Al-LAC) were investigated for the adsorption of Fe(III) from aqueous solution. Scanning electron microscopy, Fourier transform infrared, and N_2 adsorption–desorption analysis were carried out to identify adsorbents characterization. The effect of operational parameters onto the adsorption performance was investigated in batch experiments mode. The modification method significantly improves the adsorption property of activated carbon. The optimum pH was found to be 8 for all adsorbents with maximum removal efficiencies of 89.3%, 99.1%, 79.7%, and 96.7% using CAC, Al-CAC, LAC, and Al-LAC, respectively, after a contact time of 5 min and initial iron concentration of 5 mg/L. The maximum adsorption capacity was 334.9, 366.7, 317.1, and 348.8 mg/g for CAC, Al-CAC, LAC, and Al-LAC, respectively, using adsorbent dosage of 0.1 g/L and initial iron concentration of 40 mg/L. The adsorption data fit well with Langmuir model for Al-CAC, Freundlich model for CAC and Al-LAC and Dubinin–Radushkevich model for LAC. The experimental data fitted well with the pseudo-second-order model (R^2 = 0.999). The thermodynamic study confirmed the spontaneity with increased randomness of the adsorption process. The results showed that the prepared activated carbons are effective low-cost adsorbents for Fe(III) removal from aqueous solutions.

Keywords: Adsorption; Activated carbon; Corn cobs; Iron; Luffa sponge; Wastewater

1. Introduction

The pollution of the aquatic environment by heavy metals is of great concern since it leads to serious problems for human health and for life in general [1]. Heavy metals cause severe dysfunction of the central nervous system, brain, reproductive system, kidney, and liver for humans [2]. Iron is one of the most important metals that required to be maintained below the allowable concentration's limits in water streams. Large quantities of wastewater containing various concentrations of iron are generated from different industries such as coating, car, aeronautic, and steel industries [3]. In addition, water flowing through rocks and soil dissolves minerals such as iron in the water streams and increases its concentration [4].

Heavy metals can be removed from aqueous solutions using coagulation, filtration, chemical precipitation, ion exchange, reverse osmosis, and oxidation–reduction processes [5,6]. Coagulation and chemical precipitation methods require a large amount of chemicals and further treatment of the produced sludge that contains metals and also those methods are not highly efficient [7]. Membrane filtration, ion exchange, reverse osmosis, and oxidation–reduction process have not been widely applied due to many problems such as high costs, high power consumption, and membrane fouling [8]. Adsorption is considered to be one

* Corresponding author.

of the most promising techniques for heavy metals removal, because it is simple, economic, efficient, environmental friendly, and the materials are easily available [9]. Moreover, it offers the advantage of the possibility of recovering the adsorbed metals for recycling and reuse [10]. Various kinds of adsorbents have been studied, such as activated carbon, algae, bentonite, and agricultural wastes products [11,12].

For iron removal from aqueous solutions, different materials have been investigated such as *Calabrian pine* bark wastes [13], *Streptomyces rimosus* biomass [3], chitosan beads [14], modified coir fibers [6], lignite [15], egg shells [4], *Escherichia coli* biofilm supported on kaolin [1], crude olive stones [16], pecan nutshell [17], olive stone waste [9], orange peel [18], and agrobacterium tumefacient [19].

Activated carbon has long been recognized as an effective adsorbent because of its large surface area, large number of surface-active adsorption sites, and high adsorption capacity [20]. Luffa sponge and corn cobs are low-cost materials used in activated carbon preparation. Activated carbon prepared from luffa sponge has been investigated for metals and ammonium removal from aqueous solutions [21–24]. Also, different studies have been investigated for pharmaceutical removal from aqueous solutions by activated carbon prepared from luffa sponge [25,26]. Corn cobs, agricultural solid wastes, are reused in preparation of activated carbon [27–29]. Moreover, carbon prepared from corn cobs is investigated as an adsorbent for metals and dyes removal [30–33].

It is of great importance to developing a new low-cost adsorbent material with high adsorption capacity. In the present study, activated carbon prepared from available low-cost materials such as corn cobs and luffa sponge was used as adsorbents for iron removal from aqueous solution under various operational conditions. In addition, to enhance the removal performance, a modification of the developed material by aluminum loading was studied. Furthermore, the adsorption isotherm, kinetics, and thermodynamics of activated carbons and modified activated carbons were investigated.

2. Materials and methods

2.1. Materials and chemicals

Luffa sponge was obtained from a local market in Mansoura city, Egypt. Corn cobs were obtained from farmers in Dakahlia governorate, Egypt. Phosphoric acid and aluminum chloride were used in activated carbons preparation and modifications. Distilled water and $FeCl_3$ were used to prepare a stock solution of 1,000 mg/L of Fe(III). Various concentration solutions were prepared by appropriately diluting the stock solution. The initial pH level of solutions was adjusted using 0.5 M HCI and NaOH. All the chemicals used in this experiment were of analytical grade.

2.2. Preparation of activated carbons and modifications

2.2.1. Corn cobs activated carbon

The corn cobs sample was rinsed and dried at 110°C for 12 h then it was crushed. The processed corn cobs sample was activated by steeping in H_3PO_4 (85% concentration) for 12 h. The solid–liquid ratio was 1:5 (g:mL). The sample was carbonized at 500°C for 2 h in a muffle furnace, eluted with distilled water until the pH was nearly 7, and then dried for 12 h at 110°C to develop corn cobs activated carbon (CAC). A grinder was used to grind CAC to a particle size of 150–200 mesh.

2.2.2. Modified corn cobs activated carbon

To obtain the modified corn cobs activated carbon (Al-CAC), the same previous steps were done with modification before the activation process. The modification step was mixing the crushed corn cobs with 0.01 mol/L $AlCl_3$ solution for 10 h at 80°C and then filtered with filter paper and dried for 12 h at 110°C. Then the activation and carbonization processes were carried out.

2.2.3. Luffa activated carbon and modified luffa activated carbon

The preparation of luffa activated carbon (LAC) is the same as CAC preparation. While, modified luffa activated carbon (Al-LAC) was prepared as Al-CAC preparation, which was discussed in the previous section.

2.3. Adsorbents characterization

After preparation of the four types of adsorbents (CAC, Al-CAC, LAC, and Al-LAC), each adsorbent was characterized by different techniques. Field emission scanning electron microscopy (SEM) (JEOL; JSM-6510LV, Japan) was used to observe the surface morphologies of the adsorbents. It was conducted at an accelerating voltage of 20 kV. Fourier transform infrared spectroscopy (FTIR) (Thermo Scientific Nicolet IS10, Madison, Wisconsin, USA) spectrum (400–4,000 cm^{-1}) was used to identify the functional groups in the prepared adsorbents. The pellet was prepared by mixing 0.1 mg of each sample with KBr (100 mg) in a mortar pestle and resultant mixtures squeezed in a hydraulic pump. The specific surface area and the average particle size were determined by N_2 adsorption–desorption method.

2.4. Adsorption study

To determine the optimum conditions for Fe(III) removal by different adsorbents from aqueous solution, batch adsorption experiments were carried out in a 200 mL conical flasks using a magnetic stirrer with stirring rate of 150 rpm. The effects of contact time (0–30 min), temperature (20°C–45°C), initial Fe(III) concentration (5–40 mg/L), adsorbent dosage (0.01–2 g/L), and initial pH (4–10) on adsorption performance were investigated. The effect of contact time on Fe(III) removal was studied using 100 mL of 10 mg/L solutions of Fe(III) agitated with 0.1 g/L of the adsorbent for different contact times (0–30 min). The effect of temperature was studied using 100 mL of 10 mg/L solutions of Fe(III) agitated with 0.1 g/L of the adsorbent at different temperatures (20°C–45°C). The effect of pH was investigated using 100 mL of 10 mg/L solutions of Fe(III) adjusted to initial pH 4–10 and agitated with 0.1 g/L of the adsorbent for 30 min. The effect of the adsorbent dose was studied by agitating 100 mL of 10 mg/L solution of Fe(III) containing

different doses of adsorbent (0.01–2.0 g/L) for 30 min. The effect of initial iron concentration was studied by agitating 100 mL solution containing different concentrations of Fe(III) (5–40 mg/L) for 30 min with 0.1 g/L of adsorbent.

After agitation, samples were collected and the solids were removed by filtration through a 0.45 μm pore size filter paper. The final metal concentration in the filtrate and the initial concentration were determined using an atomic absorption spectrometer (Varian AA240FS, Australia). The adsorption capacity q_e (mg/g) and removal efficiency of Fe(III) at equilibrium were calculated as follows:

$$q_e\left(\text{mg/g}\right)=\frac{\left(C_0-C_e\right)V}{w} \tag{1}$$

$$\text{Removal efficiency}\left(\%\right)=100\times\frac{\left(C_0-C_e\right)}{C_0} \tag{2}$$

where q_e (mg/g) is the adsorption capacity, C_0 and C_e (mg/L) are the initial and equilibrium iron concentration, respectively, V (L) is the solution volume, and w (g) is the adsorbent mass.

2.5. Adsorption isotherm

To evaluate the adsorption capacity of the adsorbents (LAC, Al-LAC, CAC, and Al-CAC) and describe the interaction between the adsorbents and the adsorbate, Langmuir, Freundlich, and Dubinin–Radushkevich (D–R) isotherm models were applied to analyze the experimental data in this study.

The linear forms of the Langmuir (Eq. (3)), Freundlich (Eq. (4)), and Dubinin–Radushkevich (D–R) (Eqs. (5)–(7)) adsorption isotherms can be expressed as follows [9,25,34]:

$$\frac{C_e}{q_e}=\frac{1}{Q_m\cdot K_L}+\frac{C_e}{Q_m} \tag{3}$$

$$\ln q_e=\ln K_F+\frac{1}{n}\ln C_e \tag{4}$$

$$\ln q_e=\ln Q_s-B\varepsilon^2 \tag{5}$$

$$\varepsilon=RT\ln\left(1+\frac{1}{C_e}\right) \tag{6}$$

$$E=\frac{1}{\sqrt{2B}} \tag{7}$$

where C_e (mg/L) is the equilibrium concentration of Fe(III) in the solution, q_e (mg/g) is the amount of Fe(III) adsorbed at equilibrium, Q_m (mg/g) is the theoretical maximum amount of Fe(III) that can be adsorbed, K_L (L/mg) is the Langmuir adsorption constant, K_F (L/mg) is the Freundlich adsorption constant, n is the intensity of the adsorption, Q_s (mg/g) is the theoretical saturation capacity, B (mol^2/J^2) is the D–R model constant, ε is the Polanyi potential, E (kJ/mol) is the mean energy of sorption, R is the universal gas constant (8.314 J/mol K), and T (K) is the temperature.

2.6. Adsorption kinetics

To investigate the adsorption mechanism, the three most widely used kinetic models, the pseudo-first-order, the pseudo-second-order, and the intraparticle diffusion models were applied to analyze the experimental data.

The linear forms of the pseudo-first-order (Eq. (8)), pseudo-second-order (Eq. (9)), and intraparticle diffusion models (Eq. (10)) can be expressed as [12,35]:

$$\log\left(q_e-q_t\right)=\log q_t-\frac{k_1}{2.303}t \tag{8}$$

$$\frac{t}{q_t}=\frac{1}{k_2q_e^2}+\frac{1}{q_e}t \tag{9}$$

$$q_t=k_dt^{0.5}+C \tag{10}$$

where q_e (mg/g) is the adsorption capacity at equilibrium, q_t (mg/g) is the adsorption capacity at time t (min), k_1 (L/min) is the pseudo-first-order kinetic constant, k_2 (g/(mg min)) is the pseudo-second-order kinetic constant, k_d (mg/(g min$^{0.5}$)) is the intraparticle diffusion rate constant, and C (mg/g) is the intercept which represents the boundary layer thickness.

2.7. Adsorption thermodynamics

The free energy change (ΔG°), the enthalpy change (ΔH°), and the entropy change (ΔS°) of Fe(III) removal can be estimated from the variations in the equilibrium constants with the temperature. The free energy change (ΔG°) is given using Eq. (11) [36].

$$\Delta G^\circ=-RT\ln\left(\rho K_c\right) \tag{11}$$

where ΔG° (kJ/mol) is the free energy change, R is the universal gas constant (8.314 J/mol K), T (K) is the temperature, ρ (g/L) is the water density, and K_c (L/g) is the thermodynamic equilibrium constant ($K_c=q_e/C_e$). ΔS° and ΔH° values of the adsorption process were calculated from the Van't Hoff equation (12).

$$\ln\left(\rho K_c\right)=\frac{\Delta S^\circ}{R}-\frac{\Delta H^\circ}{RT} \tag{12}$$

where ΔS° and ΔH° can be then deduced from the intercept (ΔS/R) and the slope (ΔH/R) of the plot of 1/T vs. ln(ρK_c).

3. Results and discussion

3.1. Adsorbents characterization

The surface images of the four prepared adsorbents were carried out by using SEM. Fig. 1 shows the SEM images of the four adsorbents (CAC, Al-CAC, LAC, and Al-LAC). As shown in Fig. 1, the external surfaces of the activated carbons have considerable numbers of pores, which are of different sizes and shapes. The surfaces of Al-CAC and Al-LAC (Figs. 1b and d) are rougher and features a higher porous structure than CAC and LAC (Figs. 1a and c) which greatly

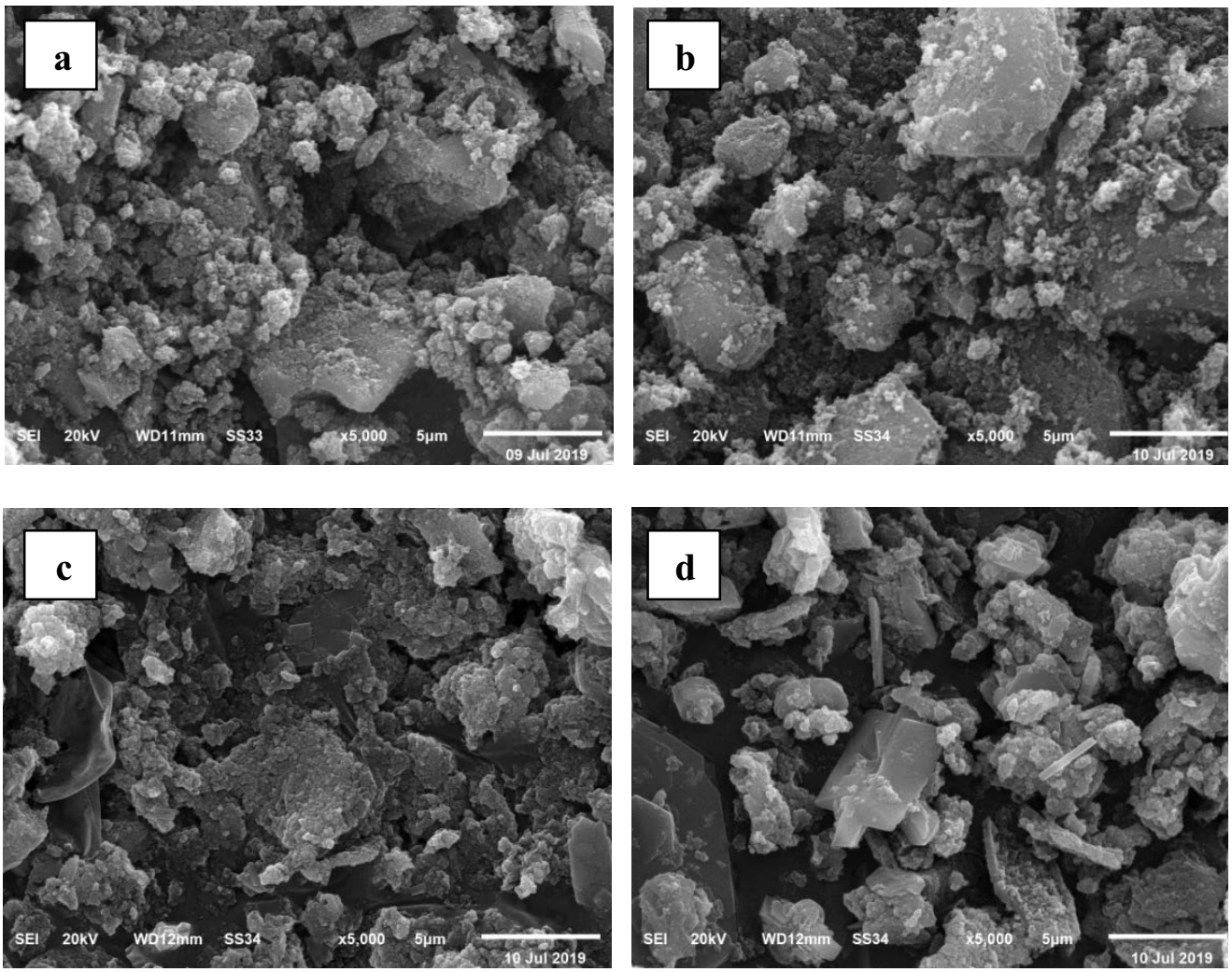

Fig. 1. SEM images of adsorbents (a) CAC, (b) Al-CAC, (c) LAC, and (d) Al-LAC.

raised its adsorption capacity. The modification process is effective in forming well-developed pores on the adsorbents surfaces, leading to Al-CAC and Al-LAC with larger surface areas and better porous structure (mesoporous). Nearly all heterogeneous types of pore structure were also distributed on the modified adsorbents surfaces.

The values of Brunauer–Emmett–Teller (BET) surface area, average pore radius, and total pore volume of the adsorbents are shown in Table 1. These values reveal that the four adsorbents may have favorable adsorption properties. AL-CAC has the highest BET surface area (146.64 m^2/g) and total pore volume (0.1868 cm^3/g) which indicates that AL-CAC has the highest capacity to remove iron ions compared to other adsorbents. The pore volume of the adsorbents corresponded to the same increasing trend as the surface area as follow: AL-CAC > AL-LAC > CAC > LAC. Therefore, the modified activated carbons with aluminum chloride (Al-CAC and Al-LAC) have high adsorption properties compared to other adsorbents.

To analyze the functional groups of the four investigated adsorbents, FTIR spectra of CAC, Al-CAC, LAC, and Al-LAC were analyzed as shown in Fig. 2. It is clear that the four adsorbents have a variety of functional groups as shown in Table 2. However, the numbers of functional groups of modified activated carbons (Al-CAC and Al-LAC) are larger than activated carbons (CAC and LAC) due to a larger number of peaks. This indicates that modified activated carbons adsorbents have a high adsorption capacity for iron.

3.2. Effect of contact time

The effect of contact time on the removal efficiency of Fe(III) using prepared activated carbons and its modifications was investigated as shown in Fig. 3. During the first minute, the removal efficiency of Fe(III) is very fast for all adsorbents. This is due to a large number of available surface sites [5]. Then the removal rate slightly increases from 1 min until it approaches equilibrium at 5 min. This is maybe attributed to the slow pore diffusion of the solute ion into the bulk of the adsorbents [20]. As shown in Fig. 3, the maximum removal efficiency achieved was 86.1%, 98.7%,

Table 1
BET surface area and pore size of the adsorbents

	CAC	AL-CAC	LAC	AL-LAC
Average pore radius (nm)	2.539	2.747	2.741	2.917
BET surface area (m^2/g)	118.53	146.64	102.08	123.14
Total pore volume (cm^3/g)	0.1505	0.1868	0.1217	0.1602

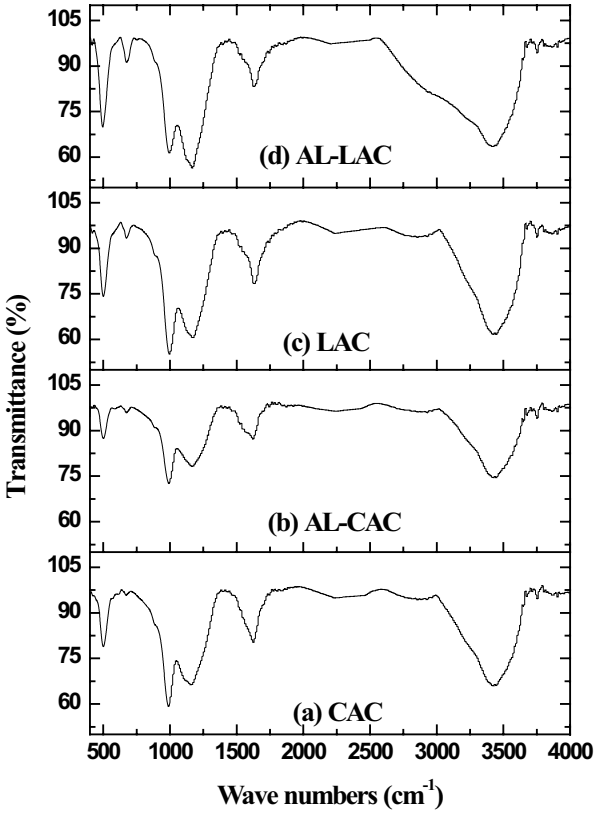

Fig. 2. FTIR spectrum of adsorbents (a) CAC, (b) Al-CAC, (c) LAC, and (d) Al-LAC.

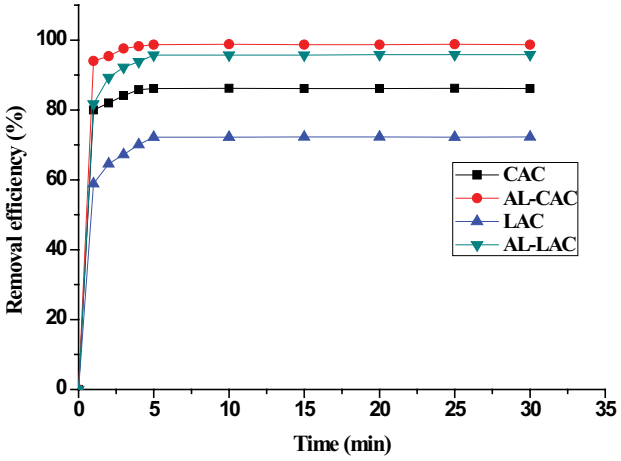

Fig. 3. Effect of contact time on the removal efficiency of Fe^{+3} (pH = 8, adsorbent dosage = 0.1 g/L, initial concentration = 10 mg/L, and temperature = 25°C).

72.2%, and 95.7% for CAC, AL-CAC, LAC, and AL-LAC, respectively after 5 min of contact time. Therefore, the modification method enhanced the removal efficiency of iron. Further increase in contact time (more than 30 min) resulted in the desorption of iron ions from the adsorbent surface.

3.3. Effect of temperature

The removal efficiency of Fe(III) by LAC and AL-LAC are affected by temperature as shown in Fig. 4. While

Table 2
Functional groups of CAC, Al-CAC, LAC, and Al-LAC adsorbents

Peaks (cm^{-1})				Functional group	References
CAC	AL-CAC	LAC	AL-LAC		
3,421–3,651–3,677–3,716–3,753–3,806–3,870–3,905–3,930	3,422–3,447–3,652–3,678–3,716–3,752–3,805–3,805–3,824–3,841–3,862–3,904–3,929	3,447–3,752–3,805–3,862–3,904	3,421–3,651–3,678–3,717–3,753–3,805–3,841–3,862–3,904–3,929	O–H and/or N–H groups	[11]
2,856–2,928	2,928–2,963	2,856	2,862	C-H vibrations	[18]
2,237	2,243	2,239	2,205	C≡C bonds	[9]
1,776–1,801–1,832	1,746–1,872	1,743	1,744–1,775–1,799–1,846–1,871	C=O stretching	[12]
1,400–1,624	1,399–1,428–1,523–1,622	1,398–1,425–1,522–1,631	1,398–1,522–1,630	Band vibration of C=C	[20]
989–1,159	992–1,166	996–1,171	995–1,167	C–O stretching	[37]
500–671	418–501–673	419–500–673	416–496–674	Metal oxygen and metal hydroxyl vibrations	[35]

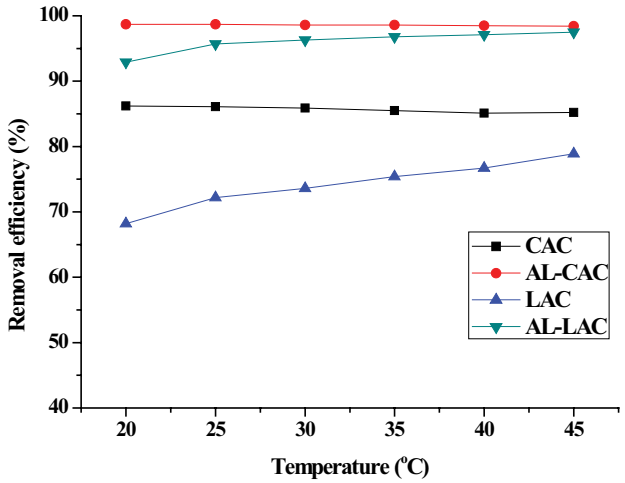

Fig. 4. Effect of temperature on the removal efficiency of Fe^{3+} (pH = 8, adsorbent dosage = 0.1 g/L, initial concentration = 10 mg/L, and contact time = 5 min).

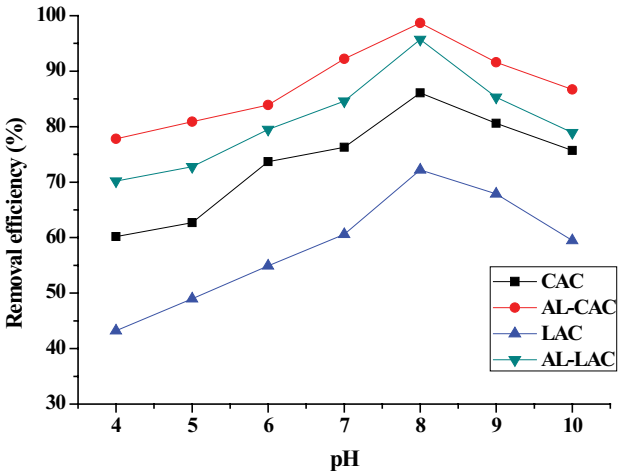

Fig. 5. Effect of pH on the removal efficiency of Fe^{3+} (adsorbent dosage = 0.1 g/L, initial concentration = 10 mg/L, contact time = 5 min, and temperature = 25°C).

temperature increases from 20°C to 45°C, the iron removal efficiency increases from 68.2% to 78.9% and 92.9% to 97.5% at equilibrium time (5 min) for LAC, and AL-LAC. This is either due to an increase in binding sites onto LAC and AL-LAC or to the higher affinity of sites for iron [38]. While, for CAC and AL-CAC, by increasing temperature from 20°C to 45°C, there is a stagnation in removal efficiency in range of 86% and 98.5%, respectively.

3.4. Effect of pH

The solution pH plays an important role in Fe(III) adsorption using the prepared activated carbons and modified activated carbons as shown in Fig. 5. The results confirmed that the sorption of iron onto adsorbents increased with increasing pH from 4 to 8 and it reached a maximum value at pH 8. This is attributed to the attraction between iron and functional groups of the adsorbents. At low pH values, the adsorbents surfaces become more positively charged which decreases the attraction between iron ions and functional groups. At high pH values, the adsorbents surfaces become more negatively charged which enhances the attraction and iron adsorption [9]. The maximum removal of Fe(III) at pH 8 is 86.1% for CAC, 98.7% for AL-CAC, 72.2% for LAC, and 95.7% for AL-LAC. For pH values higher than 8, the removal efficiency decreases again because of the competition between the formation of hydroxylated complexes of the iron and active sites on the adsorbents [19].

3.5. Effect of adsorbent dosage

The effect of adsorbent dosage on the removal efficiency of Fe(III) at pH 8 is shown in Fig. 6. While adsorbent dosage increases from 0.01 to 2 g/L, the iron removal efficiency increases from 76.9% to 89.1%, 93.7% to 99.3%, 61.1% to 79.7%, and 89.8% to 97.6% at equilibrium time equal to 5 min for CAC, AL-CAC, LAC, and AL-LAC, respectively. Nearly for all adsorbents, the removal efficiency of Fe(III) increased

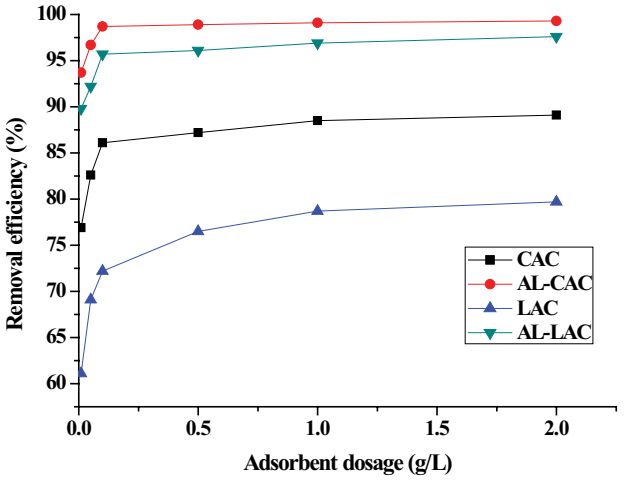

Fig. 6. Effect of adsorbent dosage on the removal efficiency of Fe^{+3} (pH = 8, initial concentration = 10 mg/L, contact time = 5 min, and temperature = 25°C).

sharply with the increase in adsorbent dosage from 0.01 to 0.1 g/L. This is attributed to an increase in available surface active sites resulting from the increased dosage of adsorbents [16]. Then the removal efficiency increased slightly with the increase in dosage from 0.1 to 2 g/L. It may be attributed to particles agglomeration and overlapping, resulting in a decrease in the availability of the surface active sites [4].

3.6. Effect of initial Fe(III) concentration

Fig. 7 shows the effect of the initial Fe(III) concentration on the removal efficiency and adsorption capacity for activated carbons and their modifications. As shown in Fig. 7a, the removal efficiency decreases from 89.3% to 34.9%, 99.1% to 66.7%, 79.7% to 17.1%, and 96.7% to 48.8% for CAC, AL-CAC, LAC, and AL-LAC, respectively, when the initial Fe(III) concentration increases from 5 to 40 mg/L.

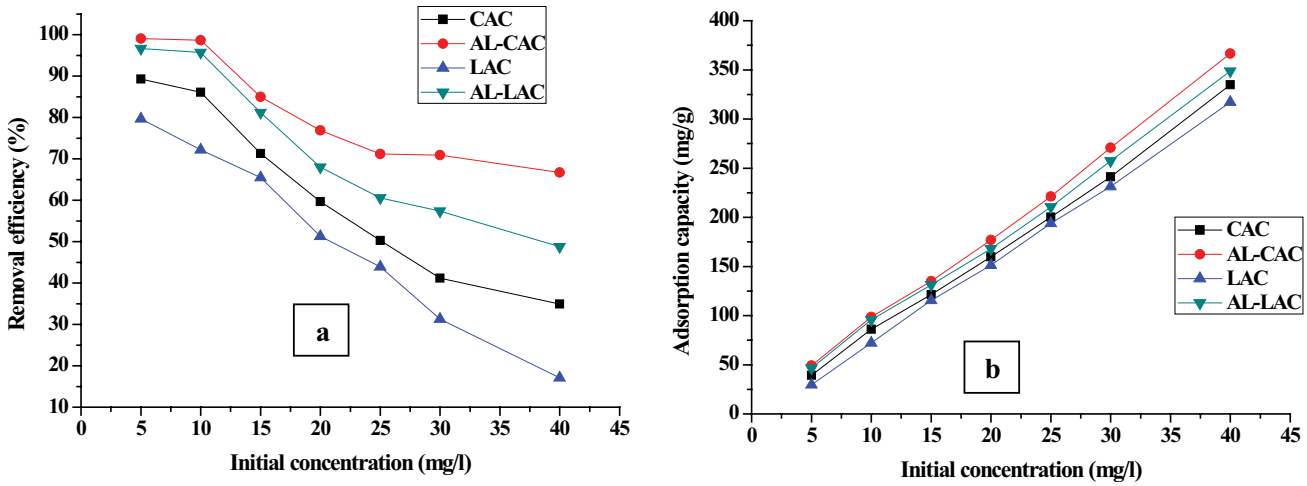

Fig. 7. Effect of initial concentration on (a) the removal efficiency and (b) adsorption capacity of Fe^{+3} (pH = 8, adsorbent dosage = 0.1 g/L, and temperature = 25°C).

This is may be due to the aggregation of iron ions at higher concentrations to large sized micelles which are difficult to diffuse through the microspores of the adsorbents [23]. While, by increasing the initial Fe(III) concentration from 5 to 40 mg/L, the adsorption capacity increases linearly from 39.3 to 334.9 mg/g, 49.1 to 366.7 mg/g, 29.7 to 317.1 mg/g, and 46.7 to 348.8 mg/g for CAC, AL-CAC, LAC, and AL-LAC, respectively, as shown in Fig. 7b. This is attributed to the increase in driving force and decrease in resistance to the uptake of solute from iron solution [16]. These results show that, the modified activated carbons (Al-CAC and Al-LAC) have the highest adsorption capacities.

3.7. Adsorption isotherm

The adsorption isotherm models were investigated for solutions with initial Fe(III) concentrations = 5–40 mg/L and adsorbent dosage = 0.1 g/L at 25°C. The results of isotherms parameters and correlation coefficients for each adsorbent were illustrated in Table 3. The Freundlich adsorption isotherm has the highest R^2 value (0.993 and 0.882) for CAC and AL-LAC, respectively. This result indicated the occurrence of multilayer adsorption on a heterogeneous surface [26]. While, the Langmuir model fits well for the adsorption of Fe(III) on AL-CAC adsorbent (R^2 = 0.867), which indicates monolayer sorption with a finite number of identical sites [20]. The adsorption of Fe(III) on LAC is obeyed to Dubinin–Radushkevich isotherm model due to the highest R^2 value (0.975) and the adsorption process is of a physical nature due to the value of E [5]. The isotherm results indicate favorable adsorption of Fe(III) onto corn cobs and luffa activated carbons and their modified activated carbons.

3.8. Comparison of investigated adsorbents with other adsorbents

In this study, the adsorption capacities (calculated from Langmuir isotherm) of various adsorbents for Fe(III) were compared in Table 4. It could be concluded that activated carbon and modified activated carbon prepared from luffa sponge and corn cobs have higher adsorption capacities than the other types of adsorbents. In addition, the adsorption of Fe(III) by activated carbons is very fast. Thus, the modified activated carbons by aluminum chloride are promising adsorbents for iron removal from an aqueous solution.

3.9. Adsorption kinetics

The pseudo-first-order, pseudo-second-order, and intraparticle diffusion kinetic models for Fe(III) adsorption by CAC, AL-CAC, LAC, and AL-LAC were illustrated in Fig. 8 and Table 5. The results for all adsorbents reveal that they had the largest correlation coefficient with respect to a pseudo-second-order equation, with R^2 of 0.999 for all adsorbents at 25°C. Compared with the other two models. Pseudo-second-order model is the most suitable model to represent the reaction and q_e (from model) is much closer to q_{exp}. This indicates that the rate-limiting step for the interaction between the adsorbent and adsorbate is chemical sorption involving valence forces through the sharing or electrons exchange [25,37].

3.10. Adsorption thermodynamics

Table 6 shows the values of $\Delta G°$, $\Delta H°$, and $\Delta S°$ for adsorption of Fe(III) on the investigated activated carbons (CAC and LAC) and their modifications (AL-CAC and AL-LAC). The negative $\Delta G°$ values at all temperatures indicate that the adsorption process is spontaneous in nature for the four adsorbents [20]. For all temperatures, $\Delta G°$ value was low (in the range from 24.30 to 34.05 kJ/mol). Thus, the adsorption low energy is characteristic of physical adsorption of iron for the four adsorbents studied [36].

The adsorption of Fe(III) onto CAC and AL-CAC has exothermic nature due to the negative $\Delta H°$ values [4]. While, the adsorption process onto LAC and AL-LAC has endothermic nature due to the positive $\Delta H°$ values [39]. The positive $\Delta S°$ values for all adsorbents confirm that there is an increase in randomness at the solid/solution interface for the adsorption of Fe(III) [12].

Table 3
Isotherms parameters for the adsorption of Fe(III) on CAC, AL-CAC, LAC, and AL-LAC

Isotherm equation	Adsorbent			
	CAC	AL-CAC	LAC	AL-LAC
		Langmuir		
Q_m (mg/g)	500	250	125	333.3
K_L (L/mg)	0.14	4.0	0.11	0.60
R^2	0.916	0.867	0.883	0.856
		Freundlich		
$1/n$	0.974	0.395	1.544	0.557
K_F (L/mg)	45.38	157.6	13.03	107.87
R^2	0.935	0.830	0.953	0.882
		Dubinin–Radushkevich		
β (mol^2/J^2)	7×10^{-7}	4×10^{-8}	2×10^{-6}	1×10^{-7}
Q_s (mg/g)	244.2	230.2	305.2	227.4
E (kJ/mol)	0.845	3.536	0.50	2.236
R^2	0.882	0.777	0.975	0.806

Table 4
Comparison of adsorption capacities of iron on different adsorbents

Adsorbent	Conditions				Q_m (mg/g)	Reference
	Fe	C_0 (mg/L)	Dose (g/L)	pH		
Corn cobs AC	III	5–40	0.1	8	500	Present study
Modified Corn cobs AC	III	5–40	0.1	8	250	Present study
Luffa sponge AC	III	5–40	0.1	8	125	Present study
Modified luffa AC	III	5–40	0.1	8	333.3	Present study
Olive stone waste AC	II	20	3	5	57.47	[9]
Cross-linked chitosan beads	III	6	0.1	5	99.09	[14]
Cross-linked chitosan beads	II	6	0.1	5	64.1	[14]
Coir fibers	II	74	20	6.6	2.84	[6]
Oxidized coir fibers	II	74	20	6	7.49	[6]
Calabrian pine bark wastes	II	55–111	10	4	2.03	[13]
Agrobacterium tumefacients	III	5–100	37.5	2.9	2.12	[19]
Pretreated orange peel	III	30	1	3	18.2	[18]
Crude olive stone	III	5–100	37.5	2.9	1.2	[16]
E. coli biofilm on kaolin	III	10–100	6.6	2.7–3.5	16.5	[1]
Streptomyces rimosus biomass	III	100	3	10	125	[3]
Pecan nutshell	III	200	4	4	76.6	[17]
Egg shells	III	1–10	2.5	7	8.7	[4]
Lignite	II	130	6	3.5	34.22	[15]
Lignite	III	130	6	3.5	11.9	[15]

4. Conclusions

In this paper, modified activated carbons prepared from corn cobs and luffa sponge are used in the adsorption of Fe(III) from aqueous solutions. Fe(III) adsorption approaches equilibrium within 5 min only and the maximum removal was favorable at pH = 8 for all adsorbents. At an adsorbent dosage of 0.1 g/L, the maximum removal efficiencies for iron were 89.3%, 99.1%, 79.7%, and 96.7% by CAC, AL-CAC, LAC, and AL-LAC, respectively, at initial iron concentration of 5 mg/L. While the maximum adsorption capacities were 334.9, 366.7, 317.1, and 348.8 mg/g for CAC, AL-CAC, LAC, and AL-LAC, respectively, at an initial iron concentration of 40 mg/L.

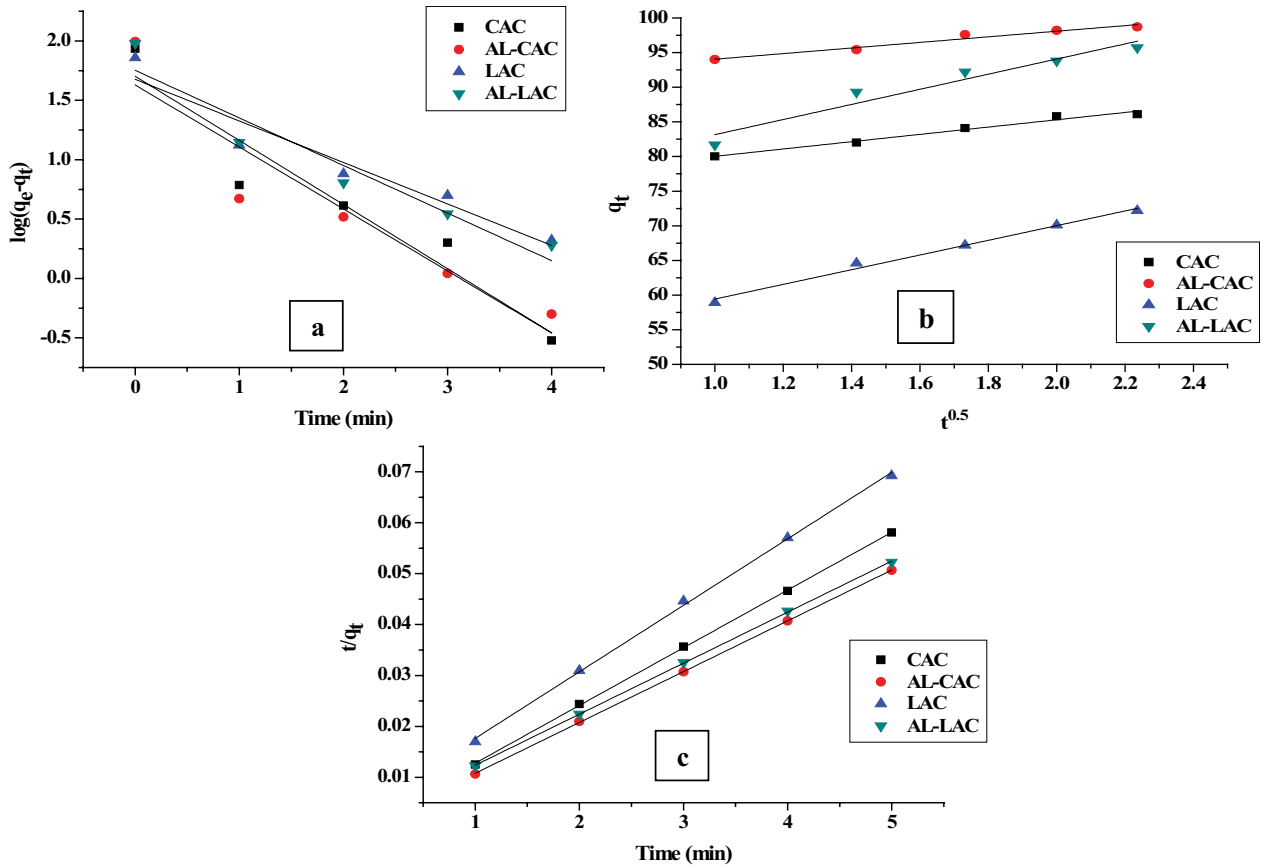

Fig. 8. Adsorption kinetic models of Fe^{3+} removal (a) pseudo-first-order, (b) pseudo-second-order, and (c) intraparticle diffusion model.

Table 5
Kinetic parameters for the adsorption of Fe(III) on CAC, AL-CAC, LAC, and AL-LAC

Kinetic model	Adsorbent			
	CAC	AL-CAC	LAC	AL-LAC
Pseudo-first-order				
k_1 (1/min)	1.244	1.202	0.804	0.921
q (mg/g)	50.35	42.56	47.42	56.49
R^2	0.921	0.885	0.931	0.923
Pseudo-second-order				
k_2 (g/(mg min))	0.121	0.10	0.042	0.05
q (mg/g)	90.91	100.0	76.92	100.0
R^2	0.999	0.999	0.999	0.999
Intraparticle diffusion				
k_d (mg/(g $min^{0.5}$))	5.27	4.034	10.59	10.91
C (mg/g)	74.76	90.01	48.84	72.24
R^2	0.980	0.963	0.990	0.942

The adsorption data fitted well Langmuir model for AL-CAC, Freundlich model for CAC and AL-LAC, and Dubinin–Radushkevich model for LAC. The adsorption kinetics fitted the pseudo-second-order model well for all adsorbents (R^2 = 0.999). The thermodynamic study confirmed the spontaneity with increased randomness of the adsorption process for all adsorbents. CAC and AL-CAC have exothermic nature but LAC and AL-LAC have endothermic nature of the adsorption process.

Table 6
Thermodynamic parameters for the adsorption of Fe(III) on CAC, AL-CAC, LAC, and AL-LAC

Parameter		Adsorbent			
		CAC	AL-CAC	LAC	AL-LAC
$\Delta H°$ (kJ/mol)		–3.03	–6.56	15.91	30.49
$\Delta S°$ (J/mol K)		81.51	90.37	137.51	203.44
$\Delta G°$(kJ/mol)	20°C	–28.72	–24.31	–33.00	–26.91
	25°C	–30.52	–25.20	–33.56	–27.35
	30°C	–31.43	–25.80	–33.94	–27.76
	35°C	–32.33	–26.47	–34.49	–28.14
	40°C	–33.12	–27.08	–34.87	–28.51
	45°C	–34.05	–27.85	–35.26	–28.99

It can be concluded that the corn cobs and luffa activated carbons are effective low-cost adsorbents for the removal of Fe(III) from aqueous solutions. Furthermore, the modification with aluminum chloride method significantly improves the adsorbent properties.

References

[1] C. Quintelas, Z. Rocha, B. Silva, B. Fonseca, H. Figueiredo, T. Tavares, Removal of Cd(II), Cr(VI), Fe(III) and Ni(II) from aqueous solutions by an *E. coli* biofilm supported on kaolin, Chem. Eng. J., 149 (2009) 319–324.

[2] Z.A. Alothman, A.H. Bahkali, M.A. Khiyami, S.M. Alfadul, S.M. Wabaidur, M. Alam, B.Z. Alfarhan, Low cost biosorbents from fungi for heavy metals removal from wastewater, Sep. Sci. Technol., 55 (2020) 1766–1775.

[3] A. Selatnia, A. Boukazoula, N. Kechid, M.Z. Bakhti, A. Chergui, Biosorption of Fe^{3+} from aqueous solution by a bacterial dead *Streptomyces rimosus* biomass, Process Biochem., 39 (2004) 1643–1651.

[4] N. Yeddou, A. Bensmaili, Equilibrium and kinetic modelling of iron adsorption by eggshells in a batch system: effect of temperature, Desalination, 206 (2007) 127–134.

[5] M. Matouq, N. Jildeh, M. Qtaishat, M. Hindiyeh, M.Q. Al Syouf, The adsorption kinetics and modeling for heavy metals removal from wastewater by Moringa pods, J. Environ. Chem. Eng., 3 (2015) 775–784.

[6] S.R. Shukla, R.S. Pai, A.D. Shendarkar, Adsorption of Ni(II), Zn(II) and Fe(II) on modified coir fibres, Sep. Purif. Technol., 47 (2006) 141–147.

[7] M. Zhao, Y. Xu, C. Zhang, H. Rong, G. Zeng, New trends in removing heavy metals from wastewater, Appl. Microbiol. Biotechnol., 100 (2016) 6509–6518.

[8] D. Mani, C. Kumar, Biotechnological advances in bioremediation of heavy metals contaminated ecosystems: an overview with special reference to phytoremediation, Int. J. Environ. Sci. Technol., 11 (2014) 843–872.

[9] T.M. Alslaibi, I. Abustan, M.A. Ahmad, A.A. Foul, Kinetics and equilibrium adsorption of iron(II), lead(II), and copper(II) onto activated carbon prepared from olive stone waste, Desal. Water Treat., 52 (2014) 7887–7897.

[10] L. Fang, L. Li, Z. Qu, H. Xu, J. Xu, N. Yan, A novel method for the sequential removal and separation of multiple heavy metals from wastewater, J. Hazard. Mater., 342 (2018) 617–624.

[11] X.S. Wang, Y.P. Tang, S.R. Tao, Kinetics, equilibrium and thermodynamic study on removal of Cr(VI) from aqueous solutions using low-cost adsorbent Alligator weed, Chem. Eng. J., 148 (2009) 217–225.

[12] X. Tang, Q. Zhang, Z. Liu, K. Pan, Y. Dong, Y. Li, Removal of Cu(II) by loofah fi bers as a natural and low-cost adsorbent from aqueous solutions, J. Mol. Liq., 199 (2014) 401–407.

[13] B. Acemioğlu, Removal of Fe(II) ions from aqueous solution by Calabrian pine bark wastes, Bioresour. Technol., 93 (2004) 99–102.

[14] W.S.W. Ngah, S. Ab Ghani, A. Kamari, Adsorption behaviour of Fe(II) and Fe(III) ions in aqueous solution on chitosan and cross-linked chitosan beads, Bioresour. Technol., 96 (2005) 443–450.

[15] D. Mohan, S. Chander, Single, binary, and multicomponent sorption of iron and manganese on lignite, J. Colloid Interface Sci., 299 (2006) 76–87.

[16] L.M. Nieto, S.B.D. Alami, G. Hodaifa, C. Faur, S. Rodriguez, J.A. Gimenez, J. Ochando, Adsorption of iron on crude olive stones, Ind. Crops Prod., 32 (2010) 467–471.

[17] J.C.P. Vaghetti, E.C. Lima, B. Royer, N.F. Cardoso, B. Martins, T. Calvete, Pecan nutshell as biosorbent to remove toxic metals from aqueous solution, Sep. Sci. Technol., 44 (2009) 615–644.

[18] V. Lugo-Lugo, C. Barrera-Díaz, F. Ureña-Núñez, B. Bilyeu, I. Linares-Hernández, Biosorption of Cr(III) and Fe(III) in single and binary systems onto pretreated orange peel, J. Environ. Manage., 112 (2012) 120–127.

[19] S. Baytak, A.R. Türker, The use of *Agrobacterium tumefacients* immobilized on Amberlite XAD-4 as a new biosorbent for the column preconcentration of iron(III), cobalt(II), manganese(II) and chromium(III), Talanta, 65 (2005) 938–945.

[20] Y.N. Wang, Q. Liu, L. Shu, M.S. Miao, Y.Z. Liu, Q. Kong, Removal of Cr(VI) from aqueous solution using Fe-modified activated carbon prepared from luffa sponge: kinetic, thermodynamic, and isotherm studies, Desal. Water Treat., 57 (2016) 29467–29478.

[21] M.S. Miao, Y.N. Wang, Q. Kong, L. Shu, Adsorption kinetics and optimum conditions for Cr(VI) removal by activated carbon prepared from luffa sponge, Desal. Water Treat., 57 (2016) 7763–7772.

[22] Y.J. Shih, C.D. Dong, Y.H. Huang, C.P. Huang, Loofah-derived activated carbon supported on nickel foam (AC/Ni) electrodes for the electro-sorption of ammonium ion from aqueous solutions, Chemosphere, 242 (2020), doi: .

[23] E.S.Z. El Ashtoukhy, *Loofa egyptiaca* as a novel adsorbent for removal of direct blue dye from aqueous solution, J. Environ. Manage., 90 (2009) 2755–2761.

[24] Z.P. Qi, Q. Liu, Z.R. Zhu, Q. Kong, Q.F. Chen, C.S. Zhao, Y.Z. Liu, M.S. Miao, C. Wang, Rhodamine B removal from aqueous solutions using loofah sponge and activated carbon prepared from loofah sponge, Desal. Water Treat., 57 (2016) 29421–29433.

[25] Q. Kong, Y.N. Wang, L. Shu, M.S. Miao, Isotherm, kinetic, and thermodynamic equations for cefalexin removal from liquids using activated carbon synthesized from loofah sponge, Desal. Water Treat., 57 (2016) 7933–7942.

[26] Q. Kong, X. He, L. Shu, M. Sheng Miao, Ofloxacin adsorption by activated carbon derived from luffa sponge: kinetic, isotherm, and thermodynamic analyses, Process Saf. Environ. Prot., 112 (2017) 254–264.

[27] Q. Cao, K.C. Xie, Y.K. Lv, W.R. Bao, Process effects on activated carbon with large specific surface area from corn cob, Bioresour. Technol., 97 (2006) 110–115.

[28] J. Kaåomierczak, P. Nowicki, R. Pietrzak, Sorption properties of activated carbons obtained from corn cobs by chemical and physical activation, Adsorption, 19 (2013) 273–281.

[29] M. Song, B. Jin, R. Xiao, L. Yang, Y. Wu, Z. Zhong, Y. Huang, The comparison of two activation techniques to prepare activated carbon from corn cob, Biomass Bioenergy, 48 (2013) 250–256.

[30] D.P. Dutta, S. Nath, Low cost synthesis of SiO_2/C nanocomposite from corn cobs and its adsorption of uranium(VI), chromium(VI) and cationic dyes from wastewater, J. Mol. Liq., 269 (2018) 140–151.

[31] S. Nethaji, A. Sivasamy, A.B. Mandal, Preparation and characterization of corn cob activated carbon coated with nano-sized magnetite particles for the removal of Cr(VI), Bioresour. Technol., 134 (2013) 94–100.

[32] X.L. Duan, C.G. Yuan, T.T. Jing, X.D. Yuan, Removal of elemental mercury using large surface area micro-porous corn cob activated carbon by zinc chloride activation, Fuel, 239 (2019) 830–840.

[33] G.O. El-Sayed, M.M. Yehia, A.A. Asaad, Assessment of activated carbon prepared from corn cob by chemical activation with phosphoric acid, Water Resour. Ind., 7–8 (2014) 66–75.

[34] L.M. Pandey, Enhanced adsorption capacity of designed bentonite and alginate beads for the effective removal of methylene blue, Appl. Clay Sci., 169 (2019) 102–111.

[35] H. Mahanna, M. Azab, Adsorption of Reactive Red 195 dye from industrial wastewater by dried soybean leaves modified with acetic acid, Desal. Water Treat., 178 (2020) 312–321.

[36] M. Bounaas, A. Bouguettoucha, D. Chebli, A. Reffas, I. Harizi, F. Rouabah, A. Amrane, High efficiency of methylene blue removal using a novel low-cost acid treated forest wastes, *Cupressus semperirens* cones: experimental results and modeling, Part. Sci. Technol., 37 (2019) 504–513.

[37] H. Younes, H. Mahanna, H.K. El-Etriby, Fast adsorption of phosphate (PO^{4-}) from wastewater using glauconite, Water Sci. Technol., 80 (2019) 1643–1653.

[38] O. Aksakal, H. Ucun, Equilibrium, kinetic and thermodynamic studies of the biosorption of textile dye (Reactive Red 195) onto *Pinus sylvestris* L., J. Hazard. Mater., 181 (2010) 666–672.

[39] G. Hodaifa, J.M. Ochando-Pulido, S. Ben Driss Alami, S. Rodriguez-Vives, A. Martinez-Ferez, Kinetic and thermodynamic parameters of iron adsorption onto olive stones, Ind. Crops Prod., 49 (2013) 526–534.